



Brain Complexity Predicts Response to Adrenocorticotrophic Hormone in Infantile Epileptic Spasms Syndrome: A Retrospective Study

Chu-Ting Zhang · Yu-Lin Sun · Wen-Bin Shi · Guang Yang ·
Chien-Hung Yeh

Received: August 11, 2022 / Accepted: October 10, 2022 / Published online: November 3, 2022
© The Author(s) 2022

ABSTRACT

Introduction: Infantile epileptic spasms syndrome (IESS) is an age-specific and severe epileptic encephalopathy. Although adrenocorticotrophic hormone (ACTH) is currently considered the preferred first-line treatment, it is not always effective and may cause side

effects. Therefore, seeking a reliable biomarker to predict the treatment response could benefit clinicians in modifying treatment options.

Methods: In this study, the complexities of electroencephalogram (EEG) recordings from 15 control subjects and 40 patients with IESS before and after ACTH therapy were retrospectively reviewed using multiscale entropy (MSE). These 40 patients were divided into responders and nonresponders according to their responses to ACTH.

Results: The EEG complexities of the patients with IESS were significantly lower than those of the healthy controls. A favorable response to treatment showed increasing complexity in the

Chu-Ting Zhang and Yu-Lin Sun contributed equally to this study as joint first authors.

Supplementary Information The online version contains supplementary material available at <https://doi.org/10.1007/s40120-022-00412-1>.

C.-T. Zhang · W.-B. Shi · C.-H. Yeh (✉)
School of Information and Electronics, Beijing
Institute of Technology, Beijing 100081, China
e-mail: nzdiw1120@gmail.com

C.-H. Yeh
Division of Interdisciplinary Medicine and
Biotechnology, Beth Israel Deaconess Medical
Center/Harvard Medical School, Boston, MA 02215,
USA

Y.-L. Sun · G. Yang (✉)
Department of Pediatrics, The First Medical Center,
Chinese PLA General Hospital, Beijing 100853,
China
e-mail: yangg301@126.com

Y.-L. Sun
Department of Plastic Surgery, Shanghai East
Hospital, Tongji University School of Medicine,
Shanghai, 200120, China

Y.-L. Sun · G. Yang
Department of Pediatrics, The Seventh Medical
Center of PLA General Hospital, Beijing 100700,
China

G. Yang
The Second School of Clinical Medicine, Southern
Medical University, Guangzhou 510280, China

γ band but exhibited a reduction in the β/α -frequency band, and again significantly elevated in the δ band, wherein the latter was prominent in the parieto-occipital regions in particular. Greater reduction in complexity was significantly linked with poorer prognosis in general. Occipital EEG complexities in the γ band revealed optimized performance in recognizing response to the treatment, corresponding to the area under the receiver operating characteristic curves as 0.8621, while complexities of the δ band served as a fair predictor of unfavorable outcomes globally.

Conclusion: We suggest that optimizing frequency-specific complexities over critical brain regions may be a promising strategy to facilitate predicting treatment response in IESS.

Keywords: Infantile epileptic spasms syndrome; Multiscale entropy; Response; Prediction; BASED score

Key Summary Points

The frequency-specific complexities over critical brain regions predict the response to adrenocorticotrophic hormone (ACTH) for epileptic spasms.

A trend of increasing, decreasing, and then rebounding in complexity correlates with a favorable prognosis.

Parieto-occipital region is a crucial brain area to access γ/δ -band complexity in recognizing response to ACTH.

General greater reduction in complexity could be a biomarker for nonresponders.

INTRODUCTION

Infantile epileptic spasms syndrome (IESS) is characterized by the onset of epileptic spasms between 1 and 24 (peak 3 and 12) months of age [1]. In the majority of patients, IESS is accompanied by intellectual disability and

developmental delay [2]. Adrenocorticotrophic hormone (ACTH) is suggested as a more effective initial treatment for children with IESS [3]. However, a retrospective study reported that almost half of infants receiving ACTH treatment failed to achieve complete remission [4]. Few studies have attempted to predict the efficacy of ACTH, and many lack reliable biomarkers to predict efficacy. The typical electroencephalogram (EEG) pattern of high-amplitude background with slow waves as well as multifocal epileptiform discharges, i.e., hypsarrhythmia, and the presence of developmental delay have been demonstrated to not be strongly related to poor prognosis [5, 6]. Very early in the course of IESS, or in older children, hypsarrhythmia may also be absent [1]. The Burden of Amplitudes and Epileptiform Discharges (BASED) score improves the poor interrater agreement of hypsarrhythmia [7]. Higher scores after ACTH treatment have been reported to be associated with higher risk of relapse [8, 9]. However, the linkage between BASED score before treatment and the potential response to the medication has been underexplored.

Since the visual EEG biomarkers are subjective, usually grounded in the consensus of clinical specialties, several quantitative computational biomarkers were introduced to aid clinicians in diagnosing children with IESS accurately [10]. Compared with controls, higher spectral power in all frequency bands during the interictal period is likely to be observed in patients with IESS [11]. The frequent occurrence of high-frequency oscillations (HFOs) was also considered a sign of IESS, yet the precise localization is still controversial, with either posterior parasagittal region [12] or frontal lobes [13] being reported as possible targets. HFO was also applied to calculate phase–amplitude coupling associated with the δ wave (3–4 Hz), where children with active epileptic spasms presented stronger coupling intensity than those with non-epileptic events [14]. However, as a predictive biomarker of treatment response, HFO failed to exhibit a robust performance to forecast the likelihood of medication response [15]. In other words, reliable objective indicators to forecast favorable outcomes of ACTH treatment for IESS are still lacking.

Entropy measures complexity, which reflects the irregularity of the neural oscillations. Loss of entropy on EEG usually accompanies aging or diseases [16], which has been demonstrated to be a promising approach to identifying neuropathological states [17–20]. Epileptic seizures are characterized by relatively high synchronization on EEG with sharp bursts in large amplitude, reflecting the clustering of millions of neurons in a structured way [21, 22], and manifesting seizure as an abnormal and organized brain state that may lead to a reduction in complexity. Multiscale entropy (MSE) quantifies the unpredictability of nonlinear oscillators, over multiple temporal and spatial scales, hence supporting richer structure quantities than those of pure sample entropy [23]. When applied to identify the abnormality of EEGs, it facilitates the detection of absence epilepsy [24] and the assessment of the outcome after brain injury [25]. Although previous studies reported that MSE measures for IESS were lower than those of healthy infants [26, 27], the linkages between dynamics in complexities over multiple frequency bands and the response to ACTH treatment had not been fully explored.

The main aim of this study is to explore the dynamics of multiscale entropy on EEG for patients with IESS, deriving complexity indexes over multiple frequencies to associate the responses to ACTH therapy as well as the impact of hypsarrhythmia, comparing responders with nonresponders. Next, we analyze correlations between the standard BASED score and the complexity indexes. Lastly, we perform receiver operating characteristic (ROC) curve analysis with EEG complexities before treatment as candidate features in treatment response prediction.

METHODS

Patient Eligibility

The clinical data of patients who were eligible for inclusion at the Chinese PLA General Hospital from November 2018 to November 2021 were retrospectively collected. The case group of this study was patients with IESS, and

the control group comprised children without epilepsy or neurodevelopmental disorders. The matching principle was that the subjects in the control group were no more than 1 year apart in age. We included the following four inclusion criteria: (1) all patients enrolled fit the definition of the International League Against Epilepsy (ILAE) for IESS [1]; (2) EEG data were available within 3 days before and after treatment; (3) the type and dose of anti-seizure medications (ASMs) remained unchanged within 1 month before and after treatment; (4) all patients completed 14 days of ACTH treatment and had at least 28 days of follow-up.

This retrospective study was approved by the Ethics Committee of the Chinese PLA General Hospital (S2020-337-01). This study was a retrospective cohort study, patient identity remained anonymous, and the requirement for informed consent was waived by the Ethics Committee of the Chinese PLA General Hospital owing to the observational nature of the study.

BASED Scoring

Two independent, well-trained neuroelectro-physiologists scored EEG data per the 2021 BASED scoring rules [11]. In the case of reviewers unable to reach a consensus, a third senior expert served as a tiebreaker. All study investigators were blinded to any previously recorded EEG reports and clinical outcomes. EEG data were reviewed using the Micromed EEG system (Zerman di Mogliano Veneto, Italy).

Data Recording

The analyzed data contained 16-channel EEG recordings placed over Fp1, Fp2, F3, F4, F7, F8, C3, C4, P3, P4, T3, T4, T5, T6, O1, and O2, according to the 10/20 international system. Data were re-referenced to the common average. All posttreatment data and all but two pretreatment data were originally recorded at a sampling rate of 256 Hz; the remaining 2 recordings and 20 control recordings were initially sampled at 512 Hz and downsampled to 256 Hz. A Butterworth bandpass filter of sixth

order set at 0.5–50 Hz and a notch filter at 50 Hz were applied to eliminate artifacts. A continuous EEG time series lasting 1 h or longer was captured per recording, including wakefulness and/or sleep. Data were epoched into 10-min segments during wakefulness and sleep, respectively.

Multiscale Entropy and EEG Complexity

Multiscale entropy (MSE), proposed by Costa et al. [28], is a representation revealing rich chaotic information of a time series over a wide range of time scales, quantifying complexities of an electrophysiological signal by sample entropy (SampEn). Details can be found in the supplementary material. MSE was calculated for each 10-min continuous epoch. Then, to address the limitation that the optimal SampEn of a certain time scale may be randomly varied, the complexity index (CI) [29] of each scale range of interest was derived by calculating the area under the MSE curve to evaluate multifrequency EEG complexities [30], reflecting the cumulative amount of entropy of an oscillator within a predetermined band. To obtain the CIs corresponding to a set of frequencies of interest (i.e., δ : 1–4 Hz, θ : 4–8 Hz, α : 8–13 Hz, β : 13–32 Hz, and γ : > 32 Hz), the scale axis was mapped to the frequency dimension according to the following $f = f_s/\tau$, of which f_s was the sampling rate of the original time series.

Statistical Analyses

All demographics and electrophysiology statistical analyses were conducted by SPSS 22.0 software (IBM Corp., Armonk, NY, USA) and JMP 13.0 software (JMP; SAS, Cary, NC), respectively. The clinical data were expressed either as median (interquartile range) or mean \pm standard deviation, depending on whether fitting a normal distribution, while categorical data were presented as percentages. Differences between categorical variables were analyzed using either chi-square or Fisher's exact test. Mann–Whitney test was applied for cross-group comparisons with nonparametric data.

To assess electrophysiology data, a generalized linear mixed model with the effects of treatment response and electrode positions, grouped by either period or presence of hypsarrhythmia, was applied to test the changes in the complexity indexes by treatment. Additionally, the differences in subjects were set as a random factor. Two-tailed p values were used for the test ($\alpha = 0.05$). The Steel–Dwass test was adopted for post-hoc analysis. $p < 0.05$ was regarded as significant. Bar plots were expressed as mean \pm standard error. Spearman's rank correlations between the CIs and BASED scores were based only on the 5-min EEG epochs that were used to clinically evaluate the latter. The CIs of the homologous right and left electrode positions were applied as mixed-features pairs to construct a classification tree model. The performances of the classification tree model are demonstrated using the averaged ROC curves with 4-fold cross-validation. The comparisons of ROC curves between different bands were analyzed using Kruskal–Wallis test. The area under the ROC curve (AUCs) gave an estimate of the overall discriminate ability. The EEG recordings were analyzed by MATLAB (MathWorks, Natick, MA).

RESULTS

Comparisons of Clinical Data

A total of 40 children with IESS were finally included, and normal EEG data from 15 individuals were collected retrospectively as control. According to the response to ACTH, patients were categorized into either the responder or the nonresponder group. Fifteen responders had no witnessed spasms within 3 consecutive days before the end of treatment, and showed no recurrence for at least 28 days during follow-up [31]. Demographic and clinical data are summarized in Table 1.

A total of five children in the response group had a history of neonatal disease, mainly including a history of hypoxia asphyxia, pathological jaundice, and other abnormalities, whereas eight children in the nonresponse group had a history of neonatal disease. There

Table 1 Patient demographics

Variable	Responder group (<i>n</i> = 15) Mean (SD), median [IQR], or <i>n</i> (%)	Nonresponder group (<i>n</i> = 25) Mean (SD), median [IQR], or <i>n</i> (%)	Control group (<i>n</i> = 15) Mean (SD), median [IQR], or <i>n</i> (%)	<i>p</i> value
Male	7 (46.7%)	16 (64%)	8 (53.3%)	0.336 ^a
Age (month)	11 ± 5.0	11 ± 4.7	6.5 ± 3.0	0.960 ^d
Age of onset (month)	5.9 ± 3.5	5.2 ± 3.1	NA	0.699 ^d
Treatment time interval	4 (1,7)	3 (1,5,9)	NA	0.600 ^a
Prematurity	2 (13.3%)	4 (16%)	NA	1.000 ^b
History of neonatal disease	5 (33.3%)	8 (32%)	NA	1.000 ^b
Family history of epilepsy	3 (20%)	3 (12%)	NA	0.654 ^b
Symptomatic Etiology	7 (46.7%)	14 (56%)	NA	0.336 ^a 0.425 ^b
Structural	3 (20%)	10 (40%)		
Genetic	4 (26.7%)	3 (12%)		
Structural and genetic	0	1 (4%)		
Unknown	8 (53.3%)	11 (44%)		
Number of ASMs used	2 (1.2)	3 (1.3)	NA	0.222 ^c
Received oral hormone	3 (20%)	9 (36%)	NA	0.477 ^b
Receiving vigabatrin	2 (13.3%)	11 (44%)	NA	0.080 ^b

^aChi-squared test^bFisher's exact test^cRank-sum test^dIndependent two-sample *t*-test

were five children in the responder group with a family history of epilepsy and three cases in the nonresponder group. We performed and assessed brain magnetic resonance imaging (MRI), whole-exome genetic testing, and hematuria screening for children in all cases. At the same time, we divided the etiologies into structural,

hereditary, and unknown etiologies. Approximately half of the responders (7 out of 15) had symptomatic etiologies, and 3 of them had structural etiologies, including one with focal cortical dysplasia, one with neonatal hypoxic-ischemic encephalopathy, and one with hypoglycemic encephalopathy. The other four

had hereditary etiology, including two cases of *WDR45* gene mutation and two cases of *CDKL5* gene mutation. Within the group of nonresponders, more than half (14 out of 25) had symptomatic etiologies, wherein 10 of them had structural etiologies including 3 focal cortical dysplasia, 2 neonatal hypoxic–ischemic encephalopathy, 2 hypoglycemic encephalopathy, 2 neonatal hypoxic–ischemic encephalopathy, and 1 tuberous sclerosis caused by *TSC2* gene mutation. There were three nonresponders of hereditary etiology including one case of *DEPDC5*, *STXBP1*, and *KCNH5* gene mutation. One patient had both structural and hereditary etiology, which manifests as *CHD2* mutation combined with hypoglycemic encephalopathy.

Between the responder and nonresponder groups, there were no significant differences in terms of gender, age, age of onset, treatment time interval, prematurity, history of neonatal disease, family history of epilepsy, etiology, types of antiepileptic drug, history of oral hormone therapy, or current vigabatrin therapy.

Comparisons of Complexity Indexes among Groups of Control, before and after ACTH Treatment

The MSE curves of EEG recordings between the controls and the patients with IESS without treatment were carefully compared on all 16 electrodes. The MSE curves from all electrodes share similar profiles. Figure 1 illustrates a

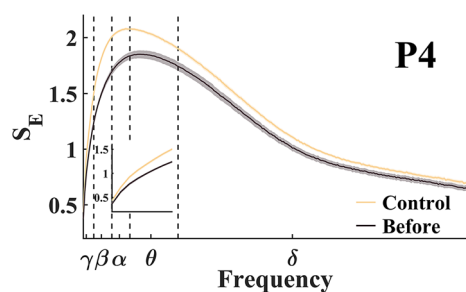


Fig. 1 The averaged MSE curves. The beige line and brownish black line represent the controls and the patients with IESS without treatment during sleep, respectively. The darker traces and the shaded areas denote mean \pm standard error

representative result of MSE on the P4 channel. Mainly, the SampEn over all scales of the control group was significantly higher than that of the “before ACTH” group.

We tested whether the CIs were affected by the treatment responses and electrode positions, grouped by the awake/sleep periods. The treatment responses had a significant effect on CI during both sleep and wakefulness across all frequency bands. Electrode positions presented a significant effect on the CIs across γ , β , θ , and δ frequencies during sleep, and across β , α , θ , and δ bands under wakefulness (Table 2). Post-hoc tests further demonstrate that CIs of the control were consistently significantly higher than those of IESS subjects in all bands (Fig. 2a–e) during sleep, regardless of whether receiving treatment, except for the δ band showing that responders exhibited CI levels comparable to those of the control. Additionally, compared with the pretreatment CIs, the responder group exhibited greater posttreatment CIs in the highest/lowest-frequency bands (i.e., γ/δ) ($p = 0.013$, right panels in Fig. 2a; $p = 0.012$, right panels in Fig. 2e) but a reduction in the mid-frequency bands (i.e., β/α) ($p = 0.027$, right panels in Fig. 2b; $p < 0.001$, right panels in Fig. 2c). In contrast, the CIs of the nonresponders were consistently lower than those of the untreated patients as well as the responders after treatment across wide frequency bands (γ , β , α , and θ bands) ($p < 0.001$, right panels in Fig. 2a–d; $p = 0.010$, right panels in Fig. 2e). During wakefulness, except for the γ band, in all frequency bands after treatment, the CIs were consistently highest in the responders after treatment, followed by the nonresponders after treatment, the controls, and the patients before treatment, all of which showed statistically significant differences, wherein the control presented the greatest CI in the γ band while no significant difference among the rest were shown.

Table 2 Generalized linear mixed model of responses to ACTH using complexity indexes (CIs) grouped by period (awake and sleep)

Period	Factor	DF	SS	F value	p value
Gamma					
Awake	Response	3	48.231	20.751	< 0.001
	Channel	15	188.906	1.060	0.391
Sleep	Response	3	574.861	173.853	< 0.001
	Channel	15	198.174	11.987	< 0.001
Beta					
Awake	Response	3	2601.506	78.027	< 0.001
	Channel	15	424.797	2.548	0.001
Sleep	Response	3	4235.619	383.545	< 0.001
	Channel	15	197.608	3.579	< 0.001
Alpha					
Awake	Response	3	4089.745	110.089	< 0.001
	Channel	15	619.817	3.337	< 0.001
Sleep	Response	3	2677.186	266.355	< 0.001
	Channel	15	59.174	1.178	0.283
Theta					
Awake	Response	3	32,752.403	135.676	< 0.001
	Channel	15	4938.654	4.092	< 0.001
Sleep	Response	3	5206.730	67.318	< 0.001
	Channel	15	819.979	2.120	0.007
Delta					
Awake	Response	3	379,321.360	109.768	< 0.001
	Channel	15	90,333.490	5.228	< 0.001
Sleep	Response	3	9688.390	5.053	0.002
	Channel	15	36,209.703	3.777	< 0.001

The factors include responses (control, responder after ACTH treatment, nonresponder after ACTH treatment, and before ACTH treatment) and electrode position (16 channels) across γ , β , α , θ , and δ bands. Bold font indicates p value < 0.05
DF degree of freedom, *SS* sum of squares

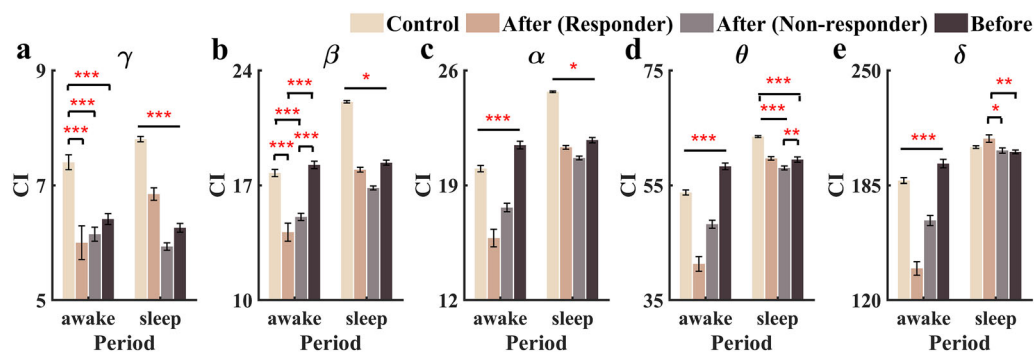


Fig. 2 Comparisons of responses to ACTH using complexity indexes (CIs). Bar plots show the CIs of control, responder to ACTH after treatment, nonresponder to ACTH after treatment, and patients before treatment across **a** γ , **b** β , **c** α , **d** θ , and **e** δ bands. All comparisons are grouped by period (awake and sleep). *, **, and *** represent

p value < 0.05, 0.01, and 0.001, respectively. The lines over the bars represent pairwise significant differences between groups, while the brackets indicate significant differences only between groups to which the brackets refer

Comparisons of Relative Changes of Complexity Indexes during the Treatment between Responder and Nonresponder to ACTH

In general, hypsarrhythmic patterns and other abnormal discharge features of IESS on EEG are more likely to emerge during sleep; thus, we included CIs only during sleep for further analyses. The absolute changes in CIs during the treatment are shown in Fig. S1. Next, we tested the topological relative changes of complexity indexes (relative CI_{b-a}) during treatment, i.e., normalized by the maximum absolute differences in CIs for the responders and nonresponders, respectively. For the non-responder group, relative CI_{b-a} exhibited a globally positive value across almost all frequency bands, whereas with the decrease of frequency, the relative CI_{b-a} of the responder group presented a trend of showing first a negative value (γ), then a positive (β/α), finally returning to a negative value (δ), in the central–posterior brain regions. Specifically, the CIs of nonresponders decreased after treatment in 15 channels, whereas the CIs of responders increased in all 14 channels except for the occipital region (O1 and O2) in the γ band (Fig. 3a). Nonresponders before treatment exhibited globally greater CIs across β , α , and θ bands (lower panels from Fig. 3b–d), whereas

the responders showed the same trend of differences in the majority of channels (except for C4) in the β/α bands (upper panels in Fig. 3b and c). For the θ band, relative CI_{b-a} of the responders turned to negative values in the central and posterior brain regions, i.e., increased CIs in the central (C3 and C4), parietal (P3 and P4), occipital (O1 and O2), and posterior-temporal (T3, T5, and T6) regions, while the six frontal electrodes remained similar to those of the β/α bands (upper panel in Fig. 3d). While the frequencies decreased to the δ band, the CIs of responders appeared to increase after treatment globally, and the CIs of nonresponders also showed an elevated trend in the parieto-occipital (P3, O1, and O2) brain regions (Fig. 3e).

The Impact of Hypsarrhythmia on Complexity Indexes by Responses to ACTH

We next tested whether the presence/absence of hypsarrhythmia affected the pretreatment CIs in identifying ACTH responses (i.e., control, responders, nonresponders) and electrode positions. The results of generalized linear mixed model analysis summarized in Table 3 demonstrate that, in the absence of hypsarrhythmia, treatment responses had significant effects (left panels in Fig. 4a–4e, left) on CIs across all

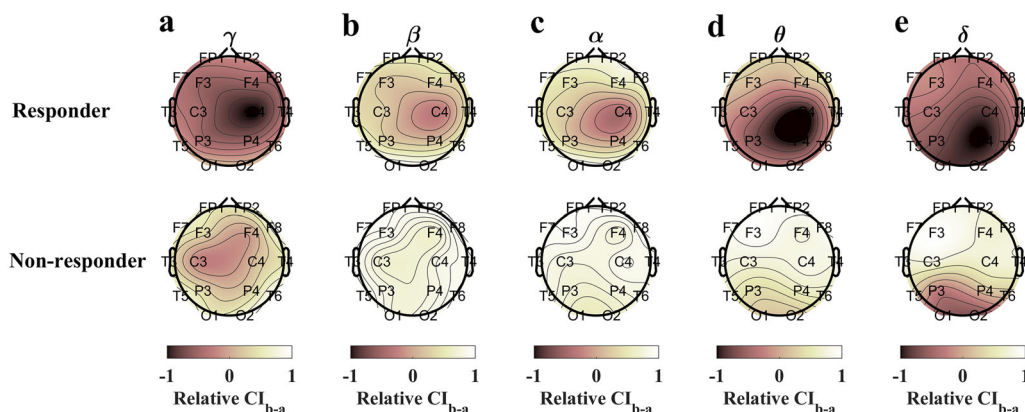


Fig. 3 Relative change of complexity indexes (relative CI_{b-a}) during treatment. The relative CI_{b-a} are normalized by the maximum absolute difference for the responders and nonresponders, respectively. Topoplots highlight the relative change across **a** γ , **b** β , **c** α , **d** θ , and **e** δ bands

frequency bands, while electrode positions had significant effects on CIs in γ , θ , and δ bands. The post-hoc tests further manifest that the effects of responses were generally consistent in the γ (Fig. 4a) and β (Fig. 4b) bands, highest in the controls and lowest in the nonresponders. With the frequencies decreased to the θ (Fig. 4d) and the δ (Fig. 4e) bands, unlike those of the γ/β ranges, the CIs of the nonresponders were significantly higher than those of the responders ($p < 0.001$, left panel in Fig. 4d; $p = 0.003$, left panel in Fig. 4e), yet both were lower than those of the control ($p < 0.001$, left panel in Fig. 4d, e).

Unlike in those without hypsarrhythmia, treatment responses had significant effects (Table 3) on CI in nearly all frequency bands except δ , whereas electrode positions had significant effects on CIs only in the γ and δ bands. The post-hoc tests further reveal that, in γ , β , α , and θ bands ($p < 0.001$, right panels in Fig. 4a–d), the CIs of control were significantly higher than those of responders and nonresponders, but not in the δ band (right panels in Fig. 4e). Of note, there was no significant difference between the responders and the nonresponders except for the α band ($p = 0.047$, right panels in Fig. 4e), where the CIs of the nonresponders were significantly higher than those of the responders.

for the responders and nonresponders. Warmer/cooler colors indicate a greater reduction/increase during treatment

Correlations between Complexities and the BASED Scores for IESS

We next explored whether there were correlations between complexities and the BASED score for patients with IESS during sleep without differentiation before/after ACTH treatment. Details can be found in the supplementary material. Only correlations with all 16 channels involved reached significant levels. Significant positive correlations between CIs of responders and the BASED scores are shown in the β and α bands (Fig. 5b; Fig. 5c), whereas a significant negative correlation is shown in the δ band (Fig. 5e). On the other side, CIs of nonresponders were positively correlated to the BASED scores in the γ , β , and α bands (Fig. 5a–c). Our results confirmed the hypothesis in general.

Classification of Responses to ACTH with Pretreatment CIs

Complexity indexes of 10-min EEG epochs during sleep were used to identify either the responders or the nonresponders to ACTH for patients with IESS by applying only EEGs prior to treatment. As per the aforementioned findings, the CIs in the γ and δ bands are essential in differentiating responses to medication for IESS. Therefore, the performances of homologous CI

Table 3 Generalized linear mixed model of responses to ACTH using complexity indexes (CIs) grouped by presence/absence of hypsarrhythmia

Hypsarrhythmia	Factor	DF	SS	F value	p value
Gamma					
Without	Response	2	266.694	190.074	< 0.001
	Channel	15	45.32	3.566	< 0.001
With	Response	2	338.152	309.404	< 0.001
	Channel	15	45.986	5.610	< 0.001
Beta					
Without	Response	2	1963.499	424.629	< 0.001
	Channel	15	28.031	0.808	0.669
With	Response	2	1768.192	379.199	< 0.001
	Channel	15	43.671	1.249	0.231
Alpha					
Without	Response	2	1390.192	387.711	< 0.001
	Channel	15	21.792	0.810	0.666
With	Response	2	1095.288	211.370	< 0.001
	Channel	15	14.296	0.368	0.986
Theta					
Without	Response	2	4514.300	205.474	< 0.001
	Channel	15	327.612	1.988	0.015
With	Response	2	1654.440	42.826	< 0.001
	Channel	15	334.910	1.156	0.303
Delta					
Without	Response	2	39,514.095	73.305	< 0.001
	Channel	15	13,175.782	3.259	< 0.001
With	Response	2	1943.643	2.634	0.073
	Channel	15	18,534.103	3.349	< 0.001

The factors include response (control, responder to ACTH before treatment, and nonresponder to ACTH before treatment) and electrode position (16 channels) across γ , β , α , θ , and δ bands. Bold font indicates p value < 0.05

DF degree of freedom, SS sum of squares

in the δ/γ bands in predicting responses to ACTH are depicted in Fig. 6. In particular, CIs over the parieto-occipital brain regions in the γ band (Fig. 6a) provided superior (AUC \geq 0.8) prediction performance for classifying the

responses to ACTH for patients with infantile spasms. Similar AUCs were also observed in the temporo-occipital brain regions in the δ band (Fig. 6b). Half brain regions showed AUCs higher than 70% for the γ -CI, and seven regions

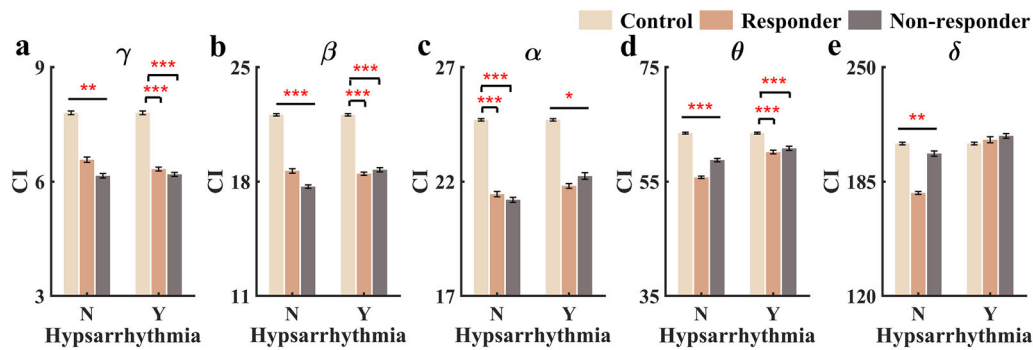


Fig. 4 Comparisons of responses to ACTH using complexity indexes (CIs) by the presence/absence of hypsarrhythmia. Bar plots show CIs of control, responder to ACTH before treatment, and nonresponder to ACTH before treatment across **a** γ , **b** β , **c** α , **d** θ , and **e** δ bands. All comparisons are grouped by the presence/absence of hypsarrhythmia. *, **, and *** represent p value < 0.05,

0.01, and 0.001, respectively. N and Y denote absence and presence of hypsarrhythmia, respectively. The lines over the bars represent pairwise significant differences between groups, while the brackets indicate significant differences only between groups to which the brackets refer

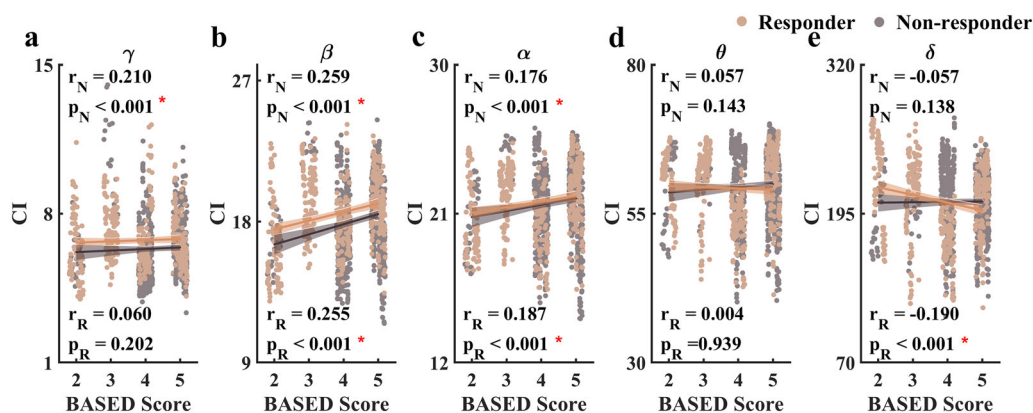


Fig. 5 Correlations between complexity indexes and BASED scores. Scatter plots depict CIs significantly correlating with the BASED scores across **a** γ , **b** β , **c** α , and **e** δ , but not **d** θ bands. * represents p value < 0.001

for the δ -CI. The sensitivity and specificity for the γ -CI in the occipital region were 78.96% and 74.75%, respectively. The sensitivity is 73.52% for the δ -CI in the occipital region, while the specificity is 74.75%. The sensitivity and specificity for the combination of these two sets of features correspond to 84.28% and 60.61%, respectively. Figure 6c depicts AUCs in classifying nonresponders and responders of 0.8621 and 0.8026, respectively, corresponding to the CIs of γ -O and δ -O. There is a significant difference between these two curves ($p = 0.025$, table S1), indicating that the predictive performance of γ -O outperformed that of δ -O.

DISCUSSION

This work developed a set of potential EEG complexity indexes in predicting a favorable outcome for patients with IESS. Considering complexities are scale dependent, for complex systems the complexity quantities require refinement to multiple time scales; of note, the scale factor in MSE analysis is negatively correlated with the frequencies on EEG [32]. Evidence showed that individuals over small scales in the complex system are relatively independent, while the larger-scale behavioral state shows the correlation of micro-individuals in

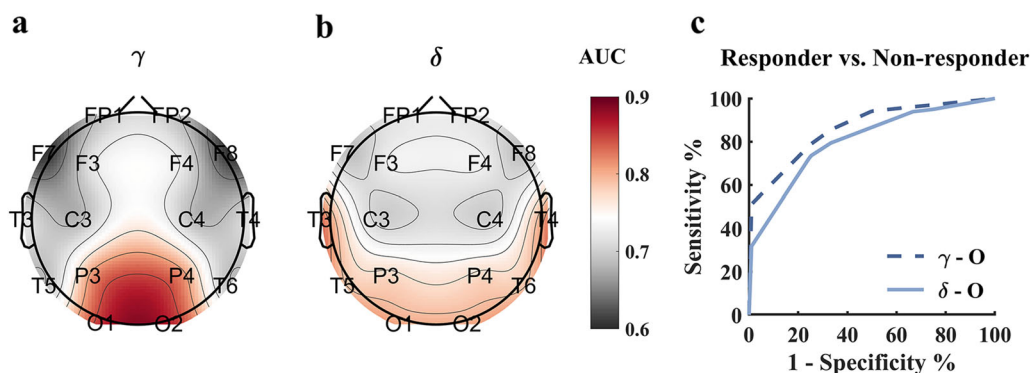


Fig. 6 Region-specific complexity predicts responses to ACTH. Brain maps illustrate the area under the curve (AUC) of the receiver operating characteristic (ROC) curve of CIs before treatment in predicting responses to ACTH across **a** γ and **b** δ bands. **c** ROC curve of

candidate features in classifying responses to ACTH for IESS. Two sets of features including γ -O CI (dashed line) and δ -O CI (solid line) were applied

the system, reducing the complexity of the system on a smaller scale [33]. In general, compared with the healthy subjects, the untreated patients had a significantly lower SampEn over a wide range of scales, which supported that higher complexity facilitated a stronger ability in adapting to uncertain changes [34]. As past studies assessed mainly a limited time scale (i.e., a high-frequency band), validating only for diagnosis but not for treatment response evaluation, comparisons of CIs over multiple frequency bands of interest were carefully examined in this study. A trend of increasing, decreasing, and then rebounding in complexity correlates with a favorable prognosis. Specifically, in the high frequencies (i.e., γ band), the CIs of the responder group after treatment were significantly higher than those before treatment, but significantly lower in the mid-frequency bands (β/α bands). In terms of the θ band, the post-treatment CIs retained a comparable level to that of before treatment, but were significantly higher after treatment in the δ band. One explanation could be that high-frequency activities are associated with interconnectivity among local neurons while low-frequency waves reflect the long-range synchronization across distributed neural populations [19]. After treatment, the local neuron adaptability of the responders increases, which could serve as a tradeoff of middle-level freedom

for enhanced cooperation of the long-scale interactions. In general, the frequency-specific complexities seem to be a promising set of indicators for a favorable outcome of IESS treatment.

The nonresponder group showed a trend of higher complexity before treatment than after treatment in the majority of frequency bands, except the δ band, which presented a comparable result to pretreatment (bottom panels in Fig. 3). The nonresponders had significantly lower complexities over all frequency bands than the responders, indicating that, regardless of partially reduced complexities during treatment either due to the tradeoff of complexities across frequencies (responders) or a relative pure pathological factor (non-responders), overall following the rule that complexity decreased with disease. The reduced complexity after treatment for the nonresponders is not altogether surprising. Evidence showed that the high functional connectivity (FC) for IESS would return to a comparable level to the controls after treatment with the responders, but excessively increase in the FC with the nonresponders [35]. These increased coherences suggest that such brains operated under a broadly synchronized state [36], leading to the reduction in SampEn. It remains uncertain why the reduced complexity is associated with a poorer prognosis, with one explanation being that

increased connectivity may lead to greater susceptibility to other seizure types [37]. The mechanism of unfavorable treatment responses to ACTH requires further exploration.

In sleep/awake complexities of healthy adults, in contrast, sleep exhibited higher entropies than awake at a short temporal scale [38], which was in line with prior research on newborn sleep [39]. A possible explanation is the incomplete myelination of the neonatal brain [40]. However, the EEG complexity under the awake state showed comparable levels to the sleep across nearly all bands of interest for the pretreatment children, likely due to complementary randomness caused by the abnormal discharges.

Next, we examined whether pretreatment CI determined ACTH responses and electrode positions in considering the presence/absence of hypsarrhythmia. Hardly significant differences were shown between the two cohorts of ACTH responses with hypsarrhythmia, supporting the existence of hypsarrhythmia before treatment failed to be an independent factor for predicting poor prognosis [10]. In contrast, the pretreatment CIs showed significant differences between the two cohorts of ACTH responses without hypsarrhythmia in the γ , θ , and δ bands, manifesting other forms of abnormal EEG characteristics, such as paroxysmal voltage attenuations, which may affect the assessment of pretreatment CIs across multiple frequency bands. In the low-frequency range (i.e., θ and δ bands), the CIs of both cohorts were significantly higher in the presence of hypsarrhythmia (Fig. S2), implying that the presence of background slow waves increased the randomness of physiological signals. In addition, correlations between the proposed complexity indexes and the BASED score for IESS were also employed, of which the BASED score was positively correlated with the CIs either for the nonresponders at $\gamma/\beta/\alpha$ bands or the responders at β/α bands, while negatively correlated with the CIs for the responders at the δ band. Although no region-specific correlation was shown, the correlations with CIs encompassing all 16 channels revealed statistical significance, supporting the BASED score reflecting a comprehensive evaluation of abnormal EEG

characteristics across multiple brain regions rather than the performance of a single electrode [11]. Hence, our view is consistent with ILAE, i.e., “Clinicians should not withhold standard therapy for children with IESS who do not have hypsarrhythmia” [1].

Our results also illustrated the distinct topographical changes in complexity during treatment between the responders and nonresponders. In general, the complexity of the responders during treatment increased in the γ band and then decreased in the β/α band globally, next presenting a reversed region-specific (central–posterior–occipital) increase in the θ band, followed by globally (also the frontal area) increased complexities in the δ band. This suggested that the central, posterior, and occipital brain regions were sensitive to the treatment responses, which was consistent with the past finding showing that long-range connections in the posterior temporal/occipital brain region were significantly reduced in the responder group of IESS [35]. Similar conclusions were shown by the performance of prediction. Region- and frequency-dependent EEG complexities before treatment classified patients into different responses to ACTH. The CI of γ -O presented the best discriminability, solidifying that the parieto-occipital region is more commonly involved in the network of epileptiform discharges [15, 41], and the γ activity exerted dominance over the posterior head area as previously reported by spectral analyses [42]. In contrast, the CIs over the δ band showed generally superior performance, supporting the stronger long-term correlations at the δ band compared with other frequencies during sleep for IESS [11]. Moreover, a previous study found that the different γ frequencies in the anterior and posterior regions might reflect differential contributions to epilepsy severity [43]. In our work, the CIs in the frontal region, especially the F3 and F4 electrodes, did poorly (AUC < 0.7) in classifying response across both γ and δ bands, which confirmed that the functional network in the frontal region lacked susceptibility to seizure outcomes.

One limitation of the current study is that we ignored the etiologies of patients with IESS patients owing to the sample size, so it remains

to be validated whether our model is generalizable across various etiologies. Second, nearly half (44%) of nonresponders to ACTH received vigabatrin, so the effect of vigabatrin on CI requires further validation. Third, owing to various reasons (e.g., neglect by parents, limited medical resources), many patients with IESS fail to receive timely treatment with ACTH; meanwhile, the initial treatment set for some patients may not be ACTH therapy. Therefore, the effect of the treatment time interval may have affected the results. In addition, as follow-up EEGs were not collected in this retrospective study, the association between long-term complexity change and development status was beyond our scope.

CONCLUSION

The complexities of the two treatment response cohorts vary in frequency and brain regions. The responders show a trend of rising, reducing, and then rebounding, along with increasing oscillation frequency, in the parieto-occipital region particularly. By contrast, the global decrease of complexities over wide frequency bands is associated with unfavorable outcomes. Our results suggest that the complexities in specific frequency bands may serve as a useful tool in predicting treatment prognosis for patients with IESS.

ACKNOWLEDGMENTS

We would like to thank the medical staff at the pediatric department of Chinese PLA Hospital for their assistance with this study.

Funding. This research was partially supported by the National Natural Science Foundation of China (No. 62171028, No. 62001026), the Natural Science Foundation of Beijing, China (No. 7222187), the Epilepsy Research Fund of China Association Against Epilepsy (No. CU-B-2021-11), the Nutrition and Care of Maternal & Child Research Fund Project of Guangzhou Biostime Institute of Nutrition &

Care (No. 2021BINCMCF030), and the BIT High-level Fellow Research Fund Program (No. 3050012222022). Chien-Hung Yeh funded the journal's Rapid Service Fee.

Author Contributions. Chu-Ting Zhang and Yu-Lin Sun wrote the first draft of the manuscript and contributed the same amount of work to the manuscript. Yu-Lin Sun performed the acquisition of data. Chu-Ting Zhang and Wen-Bin Shi performed the data analyses. Chien-Hung Yeh, Guang Yang, and Chu-Ting Zhang contributed to the conception and design of the study. All authors helped to revise the manuscript.

Disclosures. Chu-Ting Zhang, Yu-Lin Sun, Wen-Bin Shi, Guang Yang, and Chien-Hung Yeh declare no competing financial interests. We confirm that we have read the journal's position on issues involved in ethical publication and affirm that this report is consistent with those guidelines.

Compliance with Ethics Guidelines. This study was approved by the Ethics Committee of the Chinese PLA General Hospital (S2020-337-01). This study was a retrospective cohort study, patient identity remained anonymous, and the requirement for informed consent was waived by the Ethics Committee of the Chinese PLA General Hospital due to the observational nature of the study.

Data Availability Statement. The data that support the findings of this study are available from the corresponding author upon reasonable request.

Open Access. This article is licensed under a Creative Commons Attribution-NonCommercial 4.0 International License, which permits any non-commercial use, sharing, adaptation, distribution and reproduction in any medium or format, as long as you give appropriate credit to the original author(s) and the source, provide a link to the Creative Commons licence, and indicate if changes were made. The images or other third party material in this article are included in the article's Creative Commons

licence, unless indicated otherwise in a credit line to the material. If material is not included in the article's Creative Commons licence and your intended use is not permitted by statutory regulation or exceeds the permitted use, you will need to obtain permission directly from the copyright holder. To view a copy of this licence, visit <http://creativecommons.org/licenses/by-nc/4.0/>.

REFERENCES

- Zuberi SM, Wirrell E, Yozawitz E, et al. ILAE classification and definition of epilepsy syndromes with onset in neonates and infants: position statement by the ILAE Task Force on Nosology and Definitions. *Epilepsia*. 2022;63(6):1349–97.
- Hrachovy RA, Frost JD Jr. Infantile epileptic encephalopathy with hypsarrhythmia (infantile spasms/West syndrome). *J Clin Neurophysiol*. 2003;20(6):408–25.
- Grinspan ZM, Knupp KG, Patel AD, et al. Comparative effectiveness of initial treatment for infantile spasms in a contemporary US cohort. *Neurology*. 2021;97(12):e1217–28.
- Knupp KG, Coryell J, Nickels KC, et al. Response to treatment in a prospective national infantile spasms cohort. *Ann Neurol*. 2016;79(3):475–84.
- Hussain SA, Kwong G, Millichap JJ, et al. Hypsarrhythmia assessment exhibits poor interrater reliability: a threat to clinical trial validity. *Epilepsia*. 2015;56(1):77–81.
- Demarest ST, Shellhaas RA, Gaillard WD, et al. The impact of hypsarrhythmia on infantile spasms treatment response: observational cohort study from the National Infantile Spasms Consortium. *Epilepsia*. 2017;58(12):2098–103.
- Mytinger JR, Vidaurre J, Moore-Clingenpeel M, Stanek JR, Albert DVF. A reliable interictal EEG grading scale for children with infantile spasms: the 2021 BASED score. *Epilepsy Res*. 2021;173: 106631.
- Wan L, Lei YQ, Liu XT, et al. Assessing risk for relapse among children with infantile spasms using the Based score after ACTH treatment: a retrospective study. *Neurol Ther*. 2022;11(2):835–49.
- Wan L, Zhang CT, Zhu G, et al. Integration of multiscale entropy and BASED scale of electroencephalography after adrenocorticotrophic hormone therapy predict relapse of infantile spasms. *World J Pediatr*. 2022. <https://doi.org/10.1007/s12519-022-00583-9>.
- Romero Milà B, Remakanthakurup Sindhu K, Mytinger JR, Shrey DW, Lopour BA. EEG biomarkers for the diagnosis and treatment of infantile spasms. *Front Neurol*. 2022;13: 960454.
- Smith RJ, Hu DK, Shrey DW, Rajaraman R, Hussain SA, Lopour BA. Computational characteristics of interictal EEG as objective markers of epileptic spasms. *Epilepsy Res*. 2021;176: 106704.
- McCrimmon CM, Riba A, Garner C, et al. Automated detection of ripple oscillations in long-term scalp EEG from patients with infantile spasms. *J Neural Eng*. 2021;18(1):10.
- Yan L, Li L, Chen J, et al. Application of high-frequency oscillations on scalp EEG in infant spasm: a prospective controlled study. *Front Hum Neurosci*. 2021;15: 682011.
- Nariai H, Hussain SA, Bernardo D, et al. Scalp EEG interictal high frequency oscillations as an objective biomarker of infantile spasms. *Clin Neurophysiol*. 2020;131(11):2527–36.
- Bernardo D, Nariai H, Hussain SA, Sankar R, Wu JY. Interictal scalp fast ripple occurrence and high frequency oscillation slow wave coupling in epileptic spasms. *Clin Neurophysiol*. 2020;131(7):1433–43.
- Goldberger AL, Peng CK, Lipsitz LA. What is physiologic complexity and how does it change with aging and disease? *Neurobiol Aging*. 2002;23(1): 23–6.
- Deng B, Cai L, Li S, et al. Multivariate multi-scale weighted permutation entropy analysis of EEG complexity for Alzheimer's disease. *Cogn Neurodyn*. 2017;11(3):217–31.
- Gaubert S, Raimondo F, Houot M, et al. EEG evidence of compensatory mechanisms in preclinical Alzheimer's disease. *Brain*. 2019;142(7):2096–112.
- Farzan F, Atluri S, Mei Y, et al. Brain temporal complexity in explaining the therapeutic and cognitive effects of seizure therapy. *Brain*. 2017;140(4): 1011–25.
- Bosl W, Tierney A, Tager-Flusberg H, Nelson C. EEG complexity as a biomarker for autism spectrum disorder risk. *BMC Med*. 2011;9:18.
- Wang DJJ, Jann K, Fan C, et al. Neurophysiological basis of multi-scale entropy of brain complexity and its relationship with functional connectivity. *Front Neurosci*. 2018;12:352.

22. Rossini L, De Santis D, Mauceri RR, et al. Dendritic pathology, spine loss and synaptic reorganization in human cortex from epilepsy patients. *Brain*. 2021;144(1):251–65.
23. Richman JS, Moorman JR. Physiological time-series analysis using approximate entropy and sample entropy. *Am J Physiol Heart Circ Physiol*. 2000;278(6):H2039–49.
24. Weng WC, Jiang GJ, Chang CF, et al. Complexity of multi-channel electroencephalogram signal analysis in childhood absence epilepsy. *PLoS ONE*. 2015;10(8): e0134083.
25. Lu CW, Czosnyka M, Shieh JS, Smielewska A, Pickard JD, Smielewski P. Complexity of intracranial pressure correlates with outcome after traumatic brain injury. *Brain*. 2012;135(Pt 8):2399–408.
26. Chu YJ, Chang CF, Weng WC, Fan PC, Shieh JS, Lee WT. Electroencephalography complexity in infantile spasms and its association with treatment response. *Clin Neurophysiol*. 2021;132(2):480–6.
27. Lu WY, Chen JY, Chang CF, Weng WC, Lee WT, Shieh JS. Multiscale entropy of electroencephalogram as a potential predictor for the prognosis of neonatal seizures. *PLoS ONE*. 2015;10(12): e0144732.
28. Costa M, Goldberger AL, Peng CK. Multiscale entropy analysis of complex physiologic time series. *Phys Rev Lett*. 2002;89(6): 068102.
29. Manor B, Costa MD, Hu K, et al. Physiological complexity and system adaptability: evidence from postural control dynamics of older adults. *J Appl Physiol* (1985). 2010;109(6):1786–91.
30. Escudero J, Abásolo D, Hornero R, Espino P, López M. Analysis of electroencephalograms in Alzheimer's disease patients with multiscale entropy. *Physiol Meas*. 2006;27(11):1091–106.
31. Pellock JM, Hrachovy R, Shinnar S, et al. Infantile spasms: a U.S. consensus report. *Epilepsia*. 2010;51(10):2175–2189.
32. Siegenfeld AF, Bar-Yam Y, Gershenson C. An introduction to complex systems science and its applications. *Complexity*. 2020. <https://doi.org/10.1155/2020/6105872>.
33. Allen B, Stacey BC, Bar-Yam Y. Multiscale information theory and the marginal utility of information. *Entropy*. 2017;19(6):273.
34. Lin C, Yeh CH, Wang CY, et al. Robust fetal heart beat detection via R-peak intervals distribution. *IEEE Trans Biomed Eng*. 2019;66(12):3310–9.
35. Shrey DW, Kim McManus O, Rajaraman R, Ombao H, Hussain SA, Lopour BA. Strength and stability of EEG functional connectivity predict treatment response in infants with epileptic spasms. *Clin Neurophysiol*. 2018;129(10):2137–48.
36. Burroughs SA, Morse RP, Mott SH, Holmes GL. Brain connectivity in West syndrome. *Seizure*. 2014;23(7):576–9.
37. Pavone P, Striano P, Falsaperla R, Pavone L, Ruggieri M. Infantile spasms syndrome, West syndrome and related phenotypes: what we know in 2013. *Brain Dev*. 2014;36(9):739–51.
38. Shi W, Shang P, Ma Y, Sun S, Yeh CH. A comparison study on stages of sleep: quantifying multiscale complexity using higher moments on coarse-graining. *Commun Nonlinear Sci Numer Simul*. 2017;44:292–303.
39. Fraiwan L, Lweesy K. Newborn sleep stage identification using multiscale entropy. In: 2nd Middle East Conference on Biomedical Engineering; 2014, pp. 361–364.
40. McArdle CB, Richardson CJ, Nicholas DA, Mir-fakhraee M, Hayden CK, Amparo EG. Developmental features of the neonatal brain: MR imaging. Part I. Gray–white matter differentiation and myelination. *Radiology*. 1987;162(1):223–9.
41. Siniatchkin M, van Baalen A, Jacobs J, et al. Different neuronal networks are associated with spikes and slow activity in hypsarrhythmia. *Epilepsia*. 2007;48(12):2312–21.
42. Kobayashi K, Oka M, Akiyama T, et al. Very fast rhythmic activity on scalp EEG associated with epileptic spasms. *Epilepsia*. 2004;45(5):488–96.
43. Inoue T, Kobayashi K, Oka M, Yoshinaga H, Ohtsuka Y. Spectral characteristics of EEG gamma rhythms associated with epileptic spasms. *Brain Dev*. 2008;30(5):321–8.